

Impact of ^{18}F -DCFPyL PET on Staging and Treatment of Unfavorable Intermediate or High-Risk Prostate Cancer


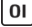
Adriano Basso Dias, MD • Antonio Finelli, MD • Glenn Bauman, MD • Patrick Veit-Haibach, MD •
Alejandro Berlin, MD • Claudia Ortega, MD • Lisa Avery, PhD • Ur Metser, MD

From the Joint Department of Medical Imaging, University Health Network, Mount Sinai Hospital & Women's College Hospital, University of Toronto, 610 University Ave, Suite 3-920, Toronto, ON, Canada M5G 2M9 (A.B.D., P.V.H., C.O., U.M.); Division of Urology, Department of Surgery (A.F.), Department of Radiation Oncology (A.B.), and Department of Biostatistics (L.A.), Princess Margaret Cancer Centre, University Health Network, University of Toronto, Toronto, Canada; and Department of Oncology, Western University, London, Canada (G.B.). Received July 19, 2021; revision requested September 13; revision received March 30, 2022; accepted April 6. **Address correspondence to** U.M. (email: Ur.metser@uhn.ca).

Study supported by Toronto General Toronto Western Hospital Foundation (NCT03535831) and the Ontario Ministry of Health and Long-Term Care provided by Ontario Health Cancer Care Ontario (NCT03718260; PREP cohort 7).

Conflicts of interest are listed at the end of this article.

See also the editorial by Jadvar in this issue.

Radiology 2022; 304:600–608 • <https://doi.org/10.1148/radiol.211836> • Content codes:  

Background: Data regarding 2-(3-{1-carboxy-5-[(6- ^{18}F)fluoro-pyridine 3-carbonyl]-amino]-pentyl}-ureido)-pentanedioic acid (^{18}F -DCFPyL) PET in primary staging of prostate cancer (PCa) are limited.

Purpose: To compare the performance of ^{18}F -DCFPyL PET/CT or PET/MRI (PET) with bone scan and CT with or without multiparametric MRI (hereafter, referred to as conventional imaging) in the initial staging of men with unfavorable intermediate or high-risk PCa and to assess treatment change after PET.

Materials and Methods: This prospective study evaluated men with biopsy-proven, untreated, unfavorable intermediate or high-risk PCa with 0 to four metastases or equivocal for extensive metastases (more than four) who underwent PET between May 2018 and December 2020. The diagnostic performance of PET in detecting pelvic nodal and distant metastases was compared with conventional imaging alone. Metastatic sites at conventional imaging and PET were compared with a composite reference standard including histopathologic analysis, correlative imaging, and/or clinical and biochemical follow-up. The intended treatment before PET was compared with the treatment plan established after performing PET. Detection rate, sensitivity, and specificity of conventional imaging and PET were compared by using McNemar exact test on paired proportions.

Results: The study consisted of 108 men (median age, 66 years; IQR, 61–73 years) with no metastases ($n = 84$), with oligometastases (four or fewer metastases; 22 men), or with equivocal findings for extensive metastases ($n = 2$). Detection rates at PET and conventional imaging for nodal metastases were 34% (37 of 108) and 11% (12 of 108) ($P < .001$), respectively, and those for distant metastases were 22% (24 of 108) and 10% (11 of 108) ($P = .02$), respectively. PET altered stage in 43 of 108 (40%) and treatment in 24 of 108 (22%) men. The most frequent treatment change was from systemic to local-regional therapy in 10 of 108 (9%) and from local-regional to systemic therapy in nine of 108 (8%) men. Equivocal findings were encountered less frequently with PET (one of 108; 1%) than with conventional imaging (29 of 108; 27%).

Conclusion: Initial staging with 2-(3-{1-carboxy-5-[(6- ^{18}F)fluoro-pyridine 3-carbonyl]-amino]-pentyl}-ureido)-pentanedioic acid (^{18}F -DCFPyL) PET after conventional imaging (bone scan and CT with or without multiparametric MRI) helped to detect more nodal and distant metastases than conventional imaging alone and changed treatment in 22% of men.

Clinical trial registration no. NCT03535831, NCT03718260

© RSNA, 2022

Online supplemental material is available for this article.

The recent proPSMA trial (1), a multicenter randomized study assessing the initial staging of men with high-risk prostate cancer (PCa) at gallium 68 (^{68}Ga)-labeled prostate-specific membrane antigen (PSMA)-11 PET/CT, showed that PET had 27% (95% CI: 23, 31) greater accuracy than bone scan and CT (hereafter, referred to as conventional imaging), fewer equivocal findings (7% vs 23%), and conferred treatment change more frequently (28% vs 15%, respectively; $P = .008$). The authors concluded that PSMA PET is a suitable replacement for conventional imaging in the primary staging of men with high-risk PCa. Clinically, both ^{68}Ga and fluorine 18 (^{18}F)-labeled PSMA-specific radiopharmaceuticals are available. ^{18}F -labeled PSMA tracers have some advantages over ^{68}Ga -labeled PSMA tracers, including

cyclotron production and a longer half-life facilitating central production and distribution (2–4). These are becoming more ubiquitous in clinical trials and clinical practice (4–6).

A second-generation ^{18}F -labeled PSMA tracer, 2-(3-{1-carboxy-5-[(6- ^{18}F)fluoro-pyridine 3-carbonyl]-amino]-pentyl}-ureido)-pentanedioic acid (^{18}F -DCFPyL) was recently approved for clinical use in the United States by the U.S. Food and Drug Administration. The diagnostic performance of this tracer was assessed previously (5–10), including two prospective multicenter clinical trials that evaluated the accuracy of ^{18}F -DCFPyL PET/CT in pelvic lymph node staging in men with PCa undergoing radical prostatectomy with pelvic lymphadenectomy (5,6). However, these studies did not compare ^{18}F -DCFPyL PET

Abbreviations

^{18}F -DCFPyL = 2-(3-{1-carboxy-5-[(6-{ ^{18}F fluoro-pyridine 3-carbonyl)-amino]-pentyl}-ureido)-pentanedioic acid, PCa = prostate cancer, PSMA = prostate-specific membrane antigen

Summary

For primary staging of unfavorable intermediate or high-risk prostate cancer, ^{18}F -DCFPyL PET helped to detect more nodal, distant metastases than did conventional imaging (bone scan, CT, and optional multiparametric MRI), altering treatment.

Key Results

- In a prospective study of 108 men with unfavorable intermediate or high-risk prostate cancer, 2-(3-{1-carboxy-5-[(6-{ ^{18}F fluoro-pyridine 3-carbonyl)-amino]-pentyl}-ureido)-pentanedioic acid (^{18}F -DCFPyL) PET helped to detect more nodal (37 vs 12 men; $P < .001$) and distant metastases (24 vs 11 men; $P = .02$) than did bone scan, CT, and optional multiparametric MRI.
- ^{18}F -DCFPyL PET helped to change staging in 43 of 108 (40%) men and treatment in 24 of 108 men (22%).
- Equivocal findings were less frequent at ^{18}F -DCFPyL PET (one of 108; 1%) than at bone scan, CT, and optional multiparametric MRI (29 of 108; 27%).

with conventional imaging, nor did they assess its effect on patient treatment. Our hypothesis was that ^{18}F -DCFPyL PET will improve rates of detection of metastatic disease in men with PCa, which would result in a change in treatment in a proportion of men. The purpose of our study was to compare the performance of ^{18}F -DCFPyL PET/CT or PET/MRI after conventional imaging to conventional imaging alone in the initial staging of men with unfavorable intermediate or high-risk PCa and to assess the impact of PET on participant treatment.

Materials and Methods

Study Design and Sample

The sample for this prospective study included men with biopsy-proven, untreated, unfavorable intermediate or high-risk PCa with 0 to four metastases or equivocal for extensive (more than four) metastases who underwent PET. Participants were enrolled between May 2018 and December 2020 from two prospective research ethics review board–approved clinical trials (*ClinicalTrials.gov*: NCT03535831, NCT03718260). Written informed consent was obtained from all participants. High-risk and unfavorable intermediate-risk stratification was according to the National Comprehensive Cancer Network guidelines (11). Within 12 weeks of enrollment, participants underwent staging at conventional imaging: contrast-enhanced abdominopelvic CT and technetium $^{99\text{m}}$ ($^{99\text{m}}\text{Tc}$)–methylene diphosphonate bone scintigraphy and optional multiparametric prostate MRI. The exclusion criteria were PCa with significant sarcomatoid or spindle cell or neuroendocrine differentiation, previous primary therapy for PCa, or presence of extensive (more than four) metastases at conventional imaging.

Imaging Protocol

^{18}F -DCFPyL was synthesized as previously described (12). PET was acquired 115 minutes \pm 16 (SD) after injection of

316 MBq \pm 15 of ^{18}F -DCFPyL with one of two imaging platforms: PET/CT or PET/MRI, as determined by one of the investigators (U.M. and P.V.H., with 19 and 17 years of experience, respectively, in PET), not blinded to clinical data and other imaging test results. PET/MRI was preferred when dedicated multiparametric MRI was clinically indicated in addition to extraprostatic staging; PET/CT was performed in other men, or when there was a contraindication to MRI. Imaging protocols for PET/CT and PET/MRI (previously described; 13), are in Tables E1–E3 (online).

Data Abstraction

Participant age, initial serum prostate-specific antigen, overall risk group category (high or unfavorable intermediate as defined by National Comprehensive Cancer Network; 11) and tumor grade according to the International Society of Urological Pathology Group Grade classification were recorded.

Conventional imaging was interpreted prospectively by a radiologist and/or nuclear medicine physician, who were not blinded to clinical data. These examinations were performed as part of screening procedures for trial inclusion. Imaging was interpreted according to standard criteria (14–16), as detailed in Appendix E1 (online). Results were abstracted independently from the clinical reports by a single body radiologist (A.B.D., with 6 years of experience), who was not blinded to clinical data. For reports lacking description of the diagnostic criteria (eg, lymph node measurements), images were reviewed again by the same radiologist to ensure the lesions conformed to the diagnostic criteria of the study. ^{18}F -DCFPyL PET/CT or PET/MRI interpretation criteria were based on the Prostate Cancer Molecular Imaging Standardized Evaluation, or PROMISE, classification, and were assigned a PSMA score and category (17,18). Maximum standardized uptake value was recorded for reference tissues (blood pool, liver, and parotid gland), primary tumor site, and metastases. PET studies were prospectively and independently reported as per the PROMISE classification by one of three readers (C.O., P.V.H., and U.M., with 11, 17, and 19 years, respectively, of PET reporting experience), who had access to all medical information including conventional imaging and prior imaging studies. Results were abstracted from the clinical reports by one unblinded radiologist (A.B.D.).

Clinical stages for pelvic nodal (N) and distant metastases (M) following the eighth edition AJCC Cancer Staging Manual were tabulated at conventional imaging and PET (19). Equivocal lesions were treated as negative findings.

Standard of Reference

A composite standard of reference was applied for all lesions identified at conventional imaging alone or after PET and included histopathologic analysis, correlative imaging, and clinical and/or biochemical follow-up (examples in Figs E1, E2 [online]). The prescription of ancillary imaging studies was at the discretion of the treating oncologist. Lesions considered to be positive findings at both conventional imaging and PET were considered to be true-positive findings for metastasis. For lesions with discrepant findings, the definition of a true-positive finding was based on the composite reference standard, including

histopathologic analysis, correlative imaging, and/or clinical or biochemical follow-up, as assessed by two reviewers (U.M. and A.B.D.), with diagnostic criteria previously defined (20–24) and detailed in Appendix E2 (online).

Assessment of Change in Treatment

The study protocol did not mandate specific participant treatment. Treatment decisions were made after review of all available clinical and imaging data by multidisciplinary genitourinary oncologists. The intended treatment plan established before PET was recorded and compared with the treatment plan or treatment received after PET. Treatment change was defined as a shift between one of the following four major modes of therapy for each participant: (a) local-regional therapy (radical prostatectomy and/or radiation with or without androgen deprivation therapy), (b) targeted therapy for oligometastatic disease (radiation therapy/surgery with or without androgen deprivation therapy), (c) systemic therapy (androgen deprivation therapy with or without chemotherapy), and (d) observation.

Statistical Analysis

Descriptive statistics were calculated for the sample, with mean \pm SD for normally distributed variables and median with range for those with skewed distributions. Overall detection rates (ie, the proportion of positive results) were calculated for conventional imaging and PET, separately for N and M stage. Sensitivity and specificity of conventional imaging and PET relative to the reference standard were evaluated. The Krippendorff α was used to assess the chance-corrected reliability in staging for PET and conventional imaging against the standard of reference and also for a subsample of participants ($n = 24$) in whom the standard of reference was on the basis of histopathologic analysis. Statistically significant differences in detection rate, sensitivity, and specificity were determined by using McNemar exact test for a test of marginal homogeneity. Logistic regression modeling (ie, univariable analyses) was used to determine factors associated with changes in stage and changes in treatment. Statistical analyses were performed (L.A., with 16 years of experience) by using statistical software (R version 4.1.0; R Foundation for Statistical Computing, www.r-project.org). Power to detect a difference in sensitivity from 0.5 to 0.7 at a prevalence of 0.73 was 73%, rising to 98% for a difference from 0.5 to 0.8 (PASS software 2021). P values less than .05 indicated statistical significance.

Results

Study Sample Characteristics

Of the 116 participants referred for staging with PET, eight men were excluded after screening (Fig 1). There were 108 men (median age, 66 years; IQR, 61–73 years) with unfavorable intermediate ($n = 21$; 19%) or high-risk ($n = 87$; 81%) PCa that met the inclusion criteria and underwent ^{18}F -DCFPyL PET/CT ($n = 54$; 50%) or PET/MRI ($n = 54$; 50%).

The primary tumor was assigned a PSMA score of 3, 2, or 1 in 65 (60%), 31 (29%) and 12 (11%) men, respectively. For reference tissues, mean maximum standardized uptake value in blood pool, liver, and parotid gland was 1.8 ± 0.6 , $7.5 \pm$

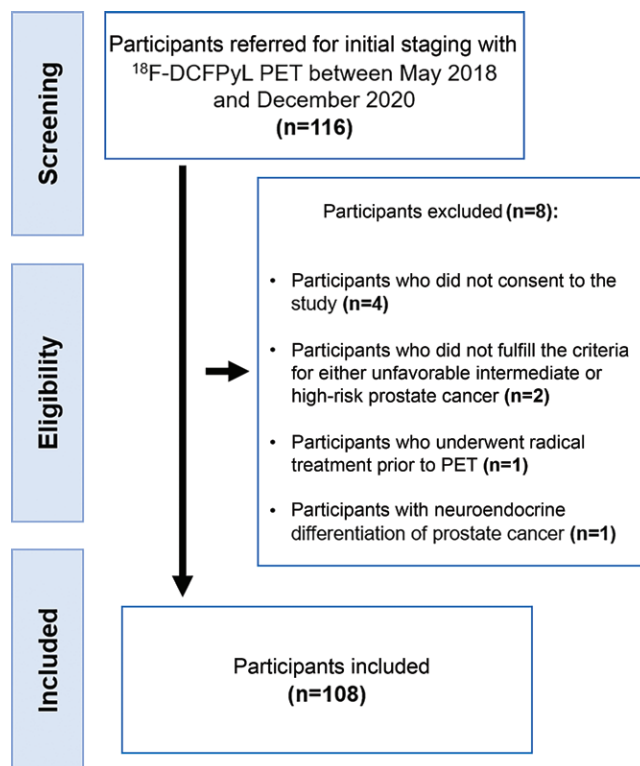


Figure 1: Participant flowchart. ^{18}F -DCFPyL = 2-(3-{1-carboxy-5-[(6-[^{18}F] fluoro-pyridine 3-carbonyl)-amino]-pentyl)-ureido)-pentanedioic acid.

1.4, and 18.7 ± 6.5 , respectively. Mean maximum standardized uptake value was 25.7 ± 19.5 (range, 2.5–102.4) for the primary tumor, 14.8 ± 15.3 (range, 2.1–84.3) for regional nodal metastases, 21.0 ± 23.1 (range, 2.1–102.4) for nonregional nodal metastases, and 14.4 ± 13.1 (range, 2.9–53.4) for bone metastases. Reference standards used are described in Table E4 (online). Lesions that could not be confirmed by the reference standard remained indeterminate. Follow-up data were available in 85 men, with a median follow-up of 13 months (range, 0–31 months). Demographic data are summarized in Table 1. According to the reference standard, there were 79 men with local-regional disease (involving the prostate with or without regional pelvic nodes) and 26 men with extraregional metastases.

Metastatic Disease at Conventional Imaging and PET

N and M stages determined at PET and conventional imaging, including CT and bone scan in all men and multiparametric MRI in 65 men, is presented in Table 2. Concordance comparison of N and M stages based on standard of reference versus conventional imaging and PET are in Tables E5 and E6 (online), respectively. PET and conventional imaging detection rate for nodal metastases was 34% (37 of 108) and 11% (12 of 108) ($P < .001$), respectively, and for distant metastases it was 22% (24 of 108) and 10% (11 of 108) ($P = .02$), respectively. Compared with the reference standard, the sensitivity of PET was higher than that of conventional imaging for pelvic nodal metastases (89% [32 of 36; 95% CI: 74, 97] vs 25% [nine of 36; 95% CI: 12, 42], respectively; $P < .001$) and for distant

metastases (92% [24 of 26; 95% CI: 75, 99] vs 23% [six of 26; 95% CI: 9, 44], respectively; $P < .001$). With equivocal lesions treated as negative findings, we found no evidence of a difference in specificity between PET and conventional imaging for nodal (100% [62 of 62; 95% CI: 94, 100] vs 97% [60 of 62; 95% CI: 89, 100], respectively; $P = .50$) or distant

metastases (100% [79 of 79; 95% CI: 86, 100] vs 96% [76 of 79; 95% CI: 89, 99], respectively; $P = .25$).

In men with histopathologic analysis as the reference standard for N stage category ($n = 24$), the specificity of PET and conventional imaging was 100% (18 of 18; 95% CI: 81, 100) and 94% (17 of 18; 95% CI: 73, 100) and the sensitivity was 50% (three of six; 95% CI: 12, 88) and 17% (1 of 6; 95% CI: 0, 64), respectively. No evidence of a difference between modalities was found for either sensitivity ($P = .5$) or specificity ($P > .99$) because of the small number of participants with discordant staging between PET and conventional imaging in this subsample.

There was poor agreement regarding N and M stages with conventional imaging and the reference standard (raw agreement, 56 of 108 [52%]; Krippendorff α , 0.15 [95% CI: -0.02, 0.31]), whereas agreement regarding N and M stages between PET and the reference standard was substantial (91 of 108 [84%]; Krippendorff α , 0.77 [95% CI: 0.66, 0.86]). For the distinction between local-regional versus distant metastatic disease, there was better agreement between PET and the reference standard (raw agreement, 103 of 108 [95%]; Krippendorff α , 0.88 [95% CI: 0.76, 0.98]) than conventional imaging and the reference standard (raw agreement, 82 of 108 [76%]; Krippendorff α , 0.22 [95% CI: -0.05, 0.46]).

Equivocal Lesions with Each Modality

Equivocal findings were encountered less frequently with PET (one of 108; 1%) than conventional imaging (29 of 108; 27%). Of the 29 men with equivocal findings at conventional imaging, nine men had regional nodal metastases only, 15 men had extraregional metastases only, and five men had both. There were 11 of 14 men (79%) with equivocal regional nodes at conventional imaging and 10 of 20 men (50%) with equivocal extraregional metastases at conventional imaging that were confirmed to be metastatic by the standard of reference. The only equivocal lesion at PET was a bone lesion, with negative findings on the standard of reference.

Table 1: Summary of Participant Characteristics

Characteristic	Value
No. of participants	108
Age (y)*	66 (61–73)
iPSA level (ng/mL)	
<10	35 (32)
10–20	24 (22)
>20	49 (45)
ISUP GG†	
1	1 (1)
2	23 (22)
3	27 (25)
4	20 (19)
5	36 (34)
Risk group	
Unfavorable intermediate risk	21 (19)
High risk	87 (81)
Metastases on conventional imaging (bone scan, CT and optional multiparametric MRI) prior to PET	
No metastases	84 (78)
Oligometastases	22 (20)
Equivocal‡	2 (2)

Note.—Unless otherwise indicated, data are numbers of participants and data in parentheses are percentages. iPSA = initial prostate-specific antigen, ISUP GG = International Society of Urological Pathology Group Grade classification.

* Data are medians, with IQR in parentheses.

† Biopsy-derived ISUP grade group (data were available for 107 patients).

‡ Equivocal for extensive metastases at conventional imaging.

Table 2: Comparison of N and M Staging with Conventional Imaging and ^{18}F -DCFPyL PET

Parameter	PET							Total
	N0M0	N0M1a	N0M1b	N1M0	N1M1a	N1M1b	N1M1c	
Conventional imaging								
N0M0	55	1	5	17	6	3	1	88
N0M1a	0	1	0	0	0	0	0	1
N0M1b	4	0	2	1	0	0	0	7
N1M0	1	0	1	5	1	1	0	9
N1M1a	1	0	0	0	0	0	0	1
N1M1b	0	0	0	0	0	2	0	2
N1M1c	0	0	0	0	0	0	0	0
Total	61	2	8	23	7	6	1	108

Note.—Data are number of participants. Conventional imaging included bone scan, CT, and optional multiparametric MRI. All patients underwent CT and bone scan; 65 patients underwent pelvic multiparametric MRI. ^{18}F -DCFPyL = 2-(3-{1-carboxy-5-[(6- ^{18}F)fluoropyridine 3-carbonyl]-amino}-pentyl)-ureido)-pentanedioic acid, N0 = no positive regional nodes, N1 = metastases in regional node (s), M0 = no distant metastases, M1a = metastases in nonregional lymph node (s), M1b = bone metastases, M1c = visceral metastases.

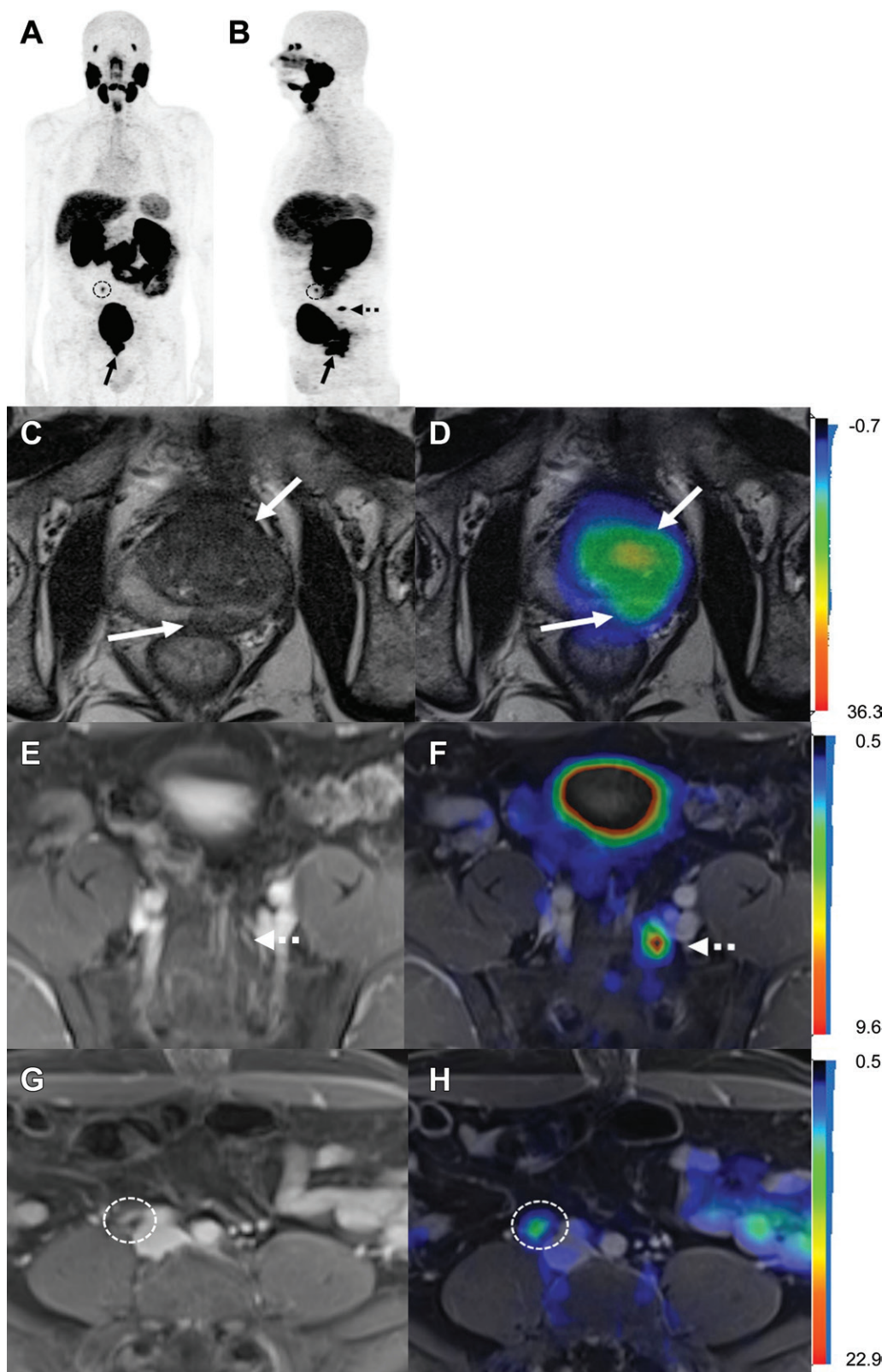


Figure 2: Images show 2-(3-[1-carboxy-5-[(6-[^{18}F] fluoro-pyridine 3-carbonyl)-amino]-pentyl]-ureido)-pentanedioic acid (^{18}F -DCFPyL) PET/MRI in a 68-year-old man with clinical T3 stage prostate cancer, International Society of Urological Pathology grade 5, with initial serum prostate-specific antigen level of 41 ng/mL. Conventional imaging (bone scan and CT; not shown) in this participant was negative for nodal or distant metastases. **(A, B)** Anteroposterior and lateral maximum intensity projection PET images show prostate-specific membrane antigen (PSMA)-avid primary tumor (solid arrows), pelvic nodal metastasis (dotted arrow), and common iliac nodal metastasis (circles). **(C)** Axial T2-weighted MRI scans in the prostate and **(D)** corresponding fused ^{18}F -DCFPyL PET/MRI in the prostate show extensive PSMA-avid primary tumor involving the transition zone and left peripheral zone of the gland (solid arrows). **(E)** Axial T1-weighted postgadolinium MRI and **(F)** corresponding fused ^{18}F -DCFPyL PET/MRI in pelvis show a small PSMA-avid left presacral lymph node (N1; dotted arrows). **(G)** Axial T1-weighted postgadolinium MRI and **(H)** corresponding fused ^{18}F -DCFPyL PET/MRI below the aortic bifurcation show a small PSMA-avid right common iliac lymph node (M1a; dotted circles). Planned local-regional treatment before the participant underwent PET was changed after undergoing PET to systemic therapy with androgen deprivation therapy.

48 men with metastases at conventional imaging and PET, respectively, oligometastatic disease was identified in 16 of 48 (33%) versus 31 of 48 (65%). Extensive metastases were identified at conventional imaging and PET, respectively, in 0 of 48 (0%) versus 12 of 48 (25%) men. There were three men with presumed oligometastatic

Impact of PET Imaging on Overall N and M Stage and Participant Treatment

PET imaging helped to alter the N and M staging in 43 of 108 participants (40%), upstaging disease extent in 36 men (33%) (Fig 2) and downstaging in seven men (7%) (Fig 3). In the

disease at conventional imaging who were shown to have extensive metastases after the addition of PET imaging.

Treatment change after PET is summarized in Table 3. Overall, PET altered treatment in 24 of 108 men (22%). The most frequent treatment changes after PET were to local-regional therapy

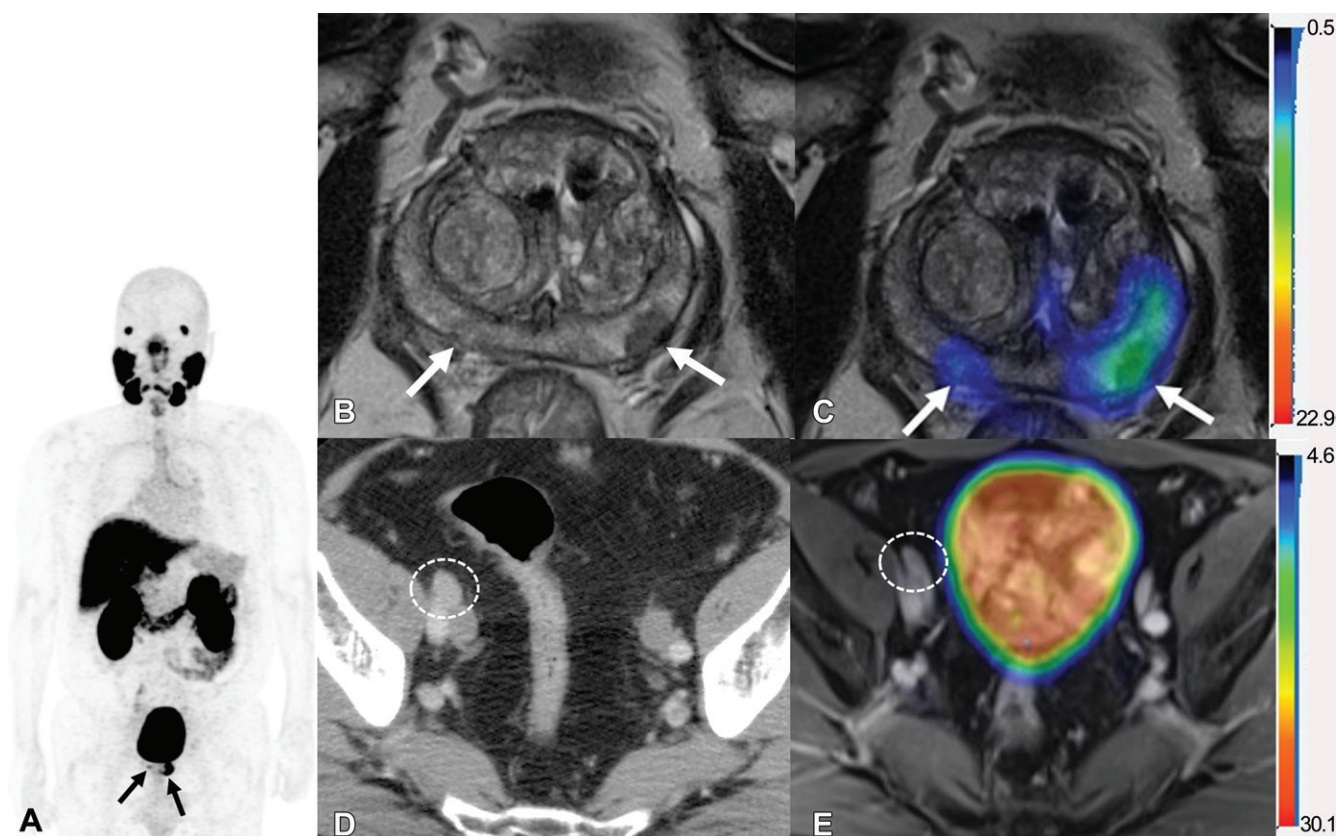


Figure 3: Images show 2-(3-{1-carboxy-5-[(6-[^{18}F] fluoro-pyridine 3-carbonyl)-amino]-pentyl}-ureido)-pentanedioic acid (^{18}F -DCFPyL) PET/MRI and contrast-enhanced CT in a 65-year-old man with clinical T3 stage prostate cancer, International Society of Urological Pathology grade group 5, with initial serum prostate-specific antigen of 19.4 ng/mL, who underwent bone scintigraphy with negative findings (not shown). **(A)** Anteroposterior maximum intensity projection image of ^{18}F -DCFPyL PET/MRI shows prostate-specific membrane antigen (PSMA)-avid primary tumor (arrows). **(B)** Axial T2-weighted MRI of the prostate and **(C)** corresponding fused ^{18}F -DCFPyL PET/MRI in the prostate show multifocal PSMA-avid primary tumors involving bilateral peripheral zone of the gland (arrows). **(D)** Axial CT image shows a 1.1 cm right external iliac lymph node, suspicious for nodal metastasis, by size criteria (N1; circle). **(E)** Axial fused ^{18}F -DCFPyL PET/MRI does not show corresponding increased tracer activity (NO; circle). At time of radical prostatectomy, lymph node sampling was negative for metastases (pT3a pN0).

Table 3: Comparison of Treatment Decisions Based on Conventional Imaging Stage and Post- ^{18}F -DCFPyL PET Stage

Parameter	PET					
	Local-regional Therapy	MDT	Systemic Therapy	Observation	NA	Total
Conventional imaging						
Local-regional Therapy	71	2	9	1	2	85
MDT	1	1	1	0	0	3
Systemic Therapy	10	0	9	0	1	20
Observation	0	0	0	0	0	0
Total	82	3	19	1	3	108

Note.—Except where indicated, data are number of participants. NA refers to no treatment decision at the time of analysis ($n = 2$); or prostate cancer therapy was deferred due to a synchronous metastatic malignancy identified on PET ($n = 1$). ^{18}F -DCFPyL = 2-(3-{1-carboxy-5-[(6-[^{18}F] fluoro-pyridine 3-carbonyl)-amino]-pentyl}-ureido)-pentanedioic acid, MDT = metastases-directed therapy, NA = not applicable.

in 11 of 108 men (10%) from planned systemic therapy mostly, and from planned local-regional therapy to systemic therapy in nine of 108 men (8%) (Fig 2). Agreement of treatment classifications before and after PET was moderate (agreement, 75%). Reliability of treatment classification was poor (Krippendorff α , 0.35; 95% CI: 0.1, 0.57).

Univariable Predictors of Change in Stage and Treatment

Univariable analyses were performed to assess predictors of change in stage and in treatment after PET (Table 4). None of these covariates were associated with change in stage. Treatment change was associated with presence of distant metastases at conventional imaging (odds ratio, 5.2; 95% CI: 1.5, 17.3).

Table 4: Univariable Analysis of Predictor of Change in Stage and in Treatment

Covariate	Stage Change		Treatment Change	
	Odds Ratio	P Value	Odds Ratio	P Value
Age	0.98 (0.93, 1.03)	.37	1.01 (0.95, 1.06)	.79
Risk group		.86		.42
Intermediate*	Reference		Reference	
High	0.91 (0.34, 2.43)		1.72 (0.46, 6.50)	
ISUP GG		.13		.36
1–2	Reference		Reference	
3	0.33 (0.09, 1.14)	.08	0.90 (0.20, 4.13)	.9
4–5	0.33 (0.11, 1.00)	.05	1.90 (0.56, 6.46)	.3
iPSA	1.00 (0.99, 1.01)	.72	0.98 (0.96, 1.00)	.11
Conventional imaging equivocal		.28		.48
No	Reference		Reference	
Yes	0.62 (0.26, 1.47)		1.43 (0.53, 3.82)	
Conventional imaging stage		.3		.001
M0	Reference		Reference	
M1	0.51 (0.15, 1.80)		10.71 (2.51, 45.67)	

Note.—Data in parentheses are 95% CIs. iPSA = initial prostate-specific antigen, ISUP GG = International Society of Urological Pathology Group Grade classification, M0 = no distant metastases, M1 = distant metastases.

* Unfavorable intermediate risk.

Discussion

Data from initial staging of prostate cancer with PET and 2-(3-{1-carboxy-5-[(6-[¹⁸F]fluoro-pyridine 3-carbonyl)-amino]-pentyl}-ureido)-pentanedioic acid (¹⁸F-DCFPyL), a second-generation fluorine 18 (¹⁸F)-labeled prostate-specific membrane antigen tracer recently approved by the U.S. Food and Drug Administration, remains limited. Our study showed that initial staging with ¹⁸F-DCFPyL PET helped to detect more nodal metastases (in 37 vs 12 men; $P < .001$) and distant metastases (in 24 vs 11 men; $P = .02$) than did CT, bone scan, and optional multiparametric MRI (hereafter, referred to as conventional imaging). Nearly one in five men initially assigned as having no metastases at conventional imaging had distant metastases at PET, and an additional one in five men had lymph node metastases at PET. Furthermore, one in four men who were suspected of having distant metastases at conventional imaging were negative for extraregional metastases according to the reference standard. Fewer equivocal findings were encountered with PET than at conventional imaging (1% vs 27%, respectively). ¹⁸F-DCFPyL PET changed staging in 40% of men and treatment in 22% of men. Presence of distant metastases at conventional imaging was a predictor of treatment change after PET. This may be explained by the detection of extensive metastases in nearly a fifth of men with presumed limited metastases, making planned metastasis-directed management inapplicable.

Our findings agree with results from previous studies (1,25), including the prospective multicenter randomized trial (pro-PSMA), reporting a sensitivity of ⁶⁸Ga-PSMA-11 PET/CT that was superior to that of conventional imaging in assessing pelvic nodal and distant metastases in high-risk PCa (85% vs 38%, respectively). A previous report (26) regarding the use of ¹⁸F-DCFPyL in the initial staging of high-risk PCa as a first-line imaging modality showed higher rates of metastases than in our study,

likely because of the exclusion of men with overt metastatic disease in our study. A unique observation in our study was the similar specificity of conventional imaging and PET for regional nodal and distant metastases. This may be because of the study inclusion criteria, where only unequivocal findings were considered to be positive findings. These results contribute to the body of literature validating the use of ¹⁸F-DCFPyL for the initial staging of men with high-risk disease. For nodal staging, compared with histopathologic analysis as the reference standard, PET had a high specificity (100%; 18 of 18) but limited sensitivity (50%; three of six). These results were in line with previously published data comparing ¹⁸F-DCFPyL PET with surgical lymph node staging (5,6) and the study by Hope et al (27), who reported a specificity of 95% and sensitivity of 40% compared with histopathologic analysis.

Overall, treatment change after PET in our study was similar to that observed in the pro-PSMA trial, in which treatment change was reported in 39 of 147 (27%) men who were crossed over to ⁶⁸Ga-PSMA-11 PET-CT after conventional imaging. In our study, curative intent local-regional therapy was offered to 10% of men who were going to undergo systemic therapy before PET. The actual treatment change may have been underestimated in our study because minor treatment changes (eg, modification of radiation therapy treatment field or extension of pelvic lymph-node dissection) were not captured. The frequent treatment change observed after PET agrees with initial results from a phase II randomized trial comparing the failure-free survival outcomes of men with high-risk PCa or biochemical failure after primary therapy by using PSMA PET/CT versus conventional imaging to guide radiation therapy (28).

Our study had limitations. First, histopathologic analysis was lacking in most participants, especially those with distant metastases or pelvic nodal metastases who underwent radiation therapy. Albeit imperfect, we used a composite reference standard,

similar to that used in other trials (1,29), which incorporated histopathologic analysis and, when not available, correlative imaging and clinical parameters including concordance between the two index tests (PET and conventional imaging) and resulting in incorporation bias and overestimation of the reported sensitivity. Nonetheless, the sensitivity observed for PET was higher than for conventional imaging compared with the same reference standard, and thus likely reflected the incremental value of ^{18}F -DCFPyL PET. Second, typical pattern of nodal metastases used when no other reference standard was available may have introduced bias in favor of PET because of the higher frequency of nodal metastases suggested with this imaging modality. However, this bias may have been limited because of the high specificity for nodal metastases compared with histopathologic analysis (30–32). Third, two different modalities (PET/CT and PET/MRI) were used. Nonetheless, the performance of ^{18}F -DCFPyL PET/CT or PET/MRI in the detection of nodal and distant metastases and its subsequent impact on treatment are similar to performances obtained from the pro-PSMA trial in which ^{68}Ga -PSMA-11 PET/CT was used.

In summary, 2-(3-{1-carboxy-5-[(6- ^{18}F]fluoro-pyridine 3-carbonyl)-amino]-pentyl}-ureido)-pentanedioic acid (^{18}F -DCFPyL) PET helped to detect more nodal and distant metastases than did conventional imaging (bone scan, CT, and optional multiparametric MRI) in men with unfavorable intermediate or high-risk prostate cancer, resulting in a change in treatment in 22% of men. Long-term follow-up and data from randomized trials are needed to determine whether this will translate to better clinical outcomes.

Author contributions: Guarantors of integrity of entire study, **A.B.D., U.M.**; study concepts/study design or data acquisition or data analysis/interpretation, all authors; manuscript drafting or manuscript revision for important intellectual content, all authors; approval of final version of submitted manuscript, all authors; agrees to ensure any questions related to the work are appropriately resolved, all authors; literature research, **A.B.D., A.F., P.V.H., U.M.**; clinical studies, **A.B.D., A.F., A.B., U.M.**; experimental studies, **A.F.**; statistical analysis, **L.A., U.M.**; and manuscript editing, all authors

Data sharing: Data generated or analyzed during the study are available from the corresponding author by request.

Disclosures of conflicts of interest: **A.B.D.** No relevant relationships. **A.F.** Participation on a DataSafety Monitoring Board or Advisory Board from Princess Margaret Cancer Center—University Health Network. **G.B.** Unrestricted research grant from Invivo Siemens. **P.V.H.** Grants from Siemens Healthineers; support for attending meetings and/or travel from Siemens Healthineers; PET Center of Excellence committee of the Society of Nuclear Medicine member. **A.B.** Participation on a DataSafety Monitoring Board or Advisory Board from Princess Margaret Cancer Center—University Health Network. **C.O.** No relevant relationships. **L.A.** No relevant relationships. **U.M.** Consulting fees from POINT Biopharm; chair, Ontario PET Steering Committee and Ontario Health-Cancer Care Ontario.

References

- Hofman MS, Lawrentschuk N, Francis RJ, et al. Prostate-specific membrane antigen PET-CT in patients with high-risk prostate cancer before curative-intent surgery or radiotherapy (proPSMA): a prospective, randomised, multicentre study. *Lancet* 2020;395(10231):1208–1216.
- Hillier SM, Maresca KP, Femia FJ, et al. Preclinical evaluation of novel glutamate-urea-lysine analogues that target prostate-specific membrane antigen as molecular imaging pharmaceuticals for prostate cancer. *Cancer Res* 2009;69(17):6932–6940.
- Chen Y, Pullambhatla M, Foss CA, et al. 2-(3-{1-Carboxy-5-[(6- ^{18}F]fluoropyridine-3-carbonyl)-amino]-pentyl-ureido)-pentanedioic acid, [^{18}F]DCFPyL, a PSMA-based PET imaging agent for prostate cancer. *Clin Cancer Res* 2011;17(24):7645–7653.
- Morris MJ, Rowe SP, Gorin MA, et al. Diagnostic performance of ^{18}F -DCFPyL-PET/CT in men with biochemically recurrent prostate cancer: Results from the CONDOR Phase III, multicenter study. *Clin Cancer Res* 2021;27(13):3674–3682.
- Pienta KJ, Gorin MA, Rowe SP, et al. A Phase 2/3 Prospective Multicenter Study of the Diagnostic Accuracy of Prostate Specific Membrane Antigen PET/CT with ^{18}F -DCFPyL in Prostate Cancer Patients (OSPREY). *J Urol* 2021;206(1):52–61.
- Jansen BHE, Bodar YJL, Zwezerijnen GJC, et al. Pelvic lymph-node staging with ^{18}F -DCFPyL PET/CT prior to extended pelvic lymph-node dissection in primary prostate cancer - the SALT trial. *Eur J Nucl Med Mol Imaging* 2021;48(2):509–520.
- Gorin MA, Rowe SP, Patel HD, et al. Prostate Specific Membrane Antigen Targeted ^{18}F -DCFPyL Positron Emission Tomography/Computerized Tomography for the Preoperative Staging of High Risk Prostate Cancer: Results of a Prospective, Phase II, Single Center Study. *J Urol* 2018;199(1):126–132.
- Parikh NR, Tsai S, Bennett C, et al. The Impact of ^{18}F -DCFPyL PET-CT Imaging on Initial Staging, Radiation, and Systemic Therapy Treatment Recommendations for Veterans With Aggressive Prostate Cancer. *Adv Radiat Oncol* 2020;5(6):1364–1369.
- Rowe SP, Macura KJ, Mena E, et al. PSMA-Based [(18) F]DCFPyL PET/CT Is Superior to Conventional Imaging for Lesion Detection in Patients with Metastatic Prostate Cancer. *Mol Imaging Biol* 2016;18(3):411–419.
- Rowe SP, Li X, Trock BJ, et al. Prospective comparison of PET imaging with PSMA-targeted ^{18}F -DCFPyL versus ^{18}F -NaF for bone lesion detection in patients with metastatic prostate cancer. *J Nucl Med* 2020;61(2):183–188.
- Mohler JL, Antonarakis ES, Armstrong AJ, et al. Prostate Cancer, Version 2.2019, NCCN Clinical Practice Guidelines in Oncology. *J Natl Compr Canc Netw* 2019;17(5):479–505.
- Ravert HT, Holt DR, Chen Y, et al. An improved synthesis of the radiolabeled prostate-specific membrane antigen inhibitor, [(18) F]DCFPyL. *J Labelled Comp Radiopharm* 2016;59(11):439–450.
- Metser U, Chan R, Veit-Haibach P, Ghai S, Tau N. Comparison of MRI sequences in whole-body PET/MRI for staging of patients with high-risk prostate cancer. *AJR Am J Roentgenol* 2019;212(2):377–381.
- Koh DM, Hughes M, Husband JE. Cross-sectional imaging of nodal metastases in the abdomen and pelvis. *Abdom Imaging* 2006;31(6):632–643.
- McMahon CJ, Rofsky NM, Pedrosa I. Lymphatic metastases from pelvic tumors: anatomic classification, characterization, and staging. *Radiology* 2010;254(1):31–46.
- Even-Sapir E, Metser U, Mishani E, Lievshitz G, Lerman H, Leibovitch I. The detection of bone metastases in patients with high-risk prostate cancer: $^{99\text{mTc}}$ -MDP Planar bone scintigraphy, single- and multi-field-of-view SPECT, ^{18}F -fluoride PET, and ^{18}F -fluoride PET/CT. *J Nucl Med* 2006;47(2):287–297.
- Eiber M, Herrmann K, Calais J, et al. Prostate cancer molecular imaging standardized evaluation (PROMISE): Proposed mTNM classification for the interpretation of PSMA-ligand PET/CT. *J Nucl Med* 2018;59(3):469–478.
- Rauscher I, Maurer T, Fendler WP, Sommer WH, Schwaiger M, Eiber M. (68) Ga -PSMA ligand PET/CT in patients with prostate cancer: How we review and report. *Cancer Imaging* 2016;16(1):14.
- Amin MB, Greene FL, Edge SB, et al. The Eighth Edition AJCC Cancer Staging Manual: Continuing to build a bridge from a population-based to a more “personalized” approach to cancer staging. *CA Cancer J Clin* 2017;67(2):93–99.
- Joniau S, Van den Bergh L, Lerut E, et al. Mapping of pelvic lymph node metastases in prostate cancer. *Eur Urol* 2013;63(3):450–458.
- Tokuda Y, Carlino LJ, Gopalan A, et al. Prostate cancer topography and patterns of lymph node metastasis. *Am J Surg Pathol* 2010;34(12):1862–1867.
- Briganti A, Suardi N, Capogrosso P, et al. Lymphatic spread of nodal metastases in high-risk prostate cancer: The ascending pathway from the pelvis to the retroperitoneum. *Prostate* 2012;72(2):186–192.
- Zacho HD, Ravn S, Afshar-Oromieh A, Fledelius J, Ejlersen JA, Petersen LJ. Added value of ^{68}Ga -PSMA PET/CT for the detection of bone metastases in patients with newly diagnosed prostate cancer and a previous $^{99\text{mTc}}$ bone scintigraphy. *EJNMMI Res* 2020;10(1):31.
- Löfgren J, Mortensen J, Rasmussen SH, et al. A Prospective Study Comparing $^{99\text{mTc}}$ -Hydroxyethylene-Diphosphonate Planar Bone Scintigraphy and Whole-Body SPECT/CT with ^{18}F -Fluoride PET/CT and ^{18}F -Fluoride PET/MRI for Diagnosing Bone Metastases. *J Nucl Med* 2017;58(11):1778–1785.
- Hirnas N, Al-Ibraheem A, Herrmann K, et al. [^{68}Ga]PSMA PET/CT Improves Initial Staging and Management Plan of Patients with High-Risk Prostate Cancer. *Mol Imaging Biol* 2019;21(3):574–581.

26. Wondergem M, van der Zant FM, Broos WAM, et al. ^{18}F -DCFPyL PET/CT for primary staging in 160 high-risk prostate cancer patients; metastasis detection rate, influence on clinical management and preliminary results of treatment efficacy. *Eur J Nucl Med Mol Imaging* 2021;48(2):521–531.
27. Hope TA, Eiber M, Armstrong WR, et al. Diagnostic Accuracy of ^{68}Ga -PSMA-11 PET for Pelvic Nodal Metastasis Detection Prior to Radical Prostatectomy and Pelvic Lymph Node Dissection: A Multicenter Prospective Phase 3 Imaging Trial. *JAMA Oncol* 2021;7(11):1635–1642.
28. Menard C, Delouya G, Wong P, et al. Randomized Controlled Trial of PSMA PET/CT Guided Intensification of Radiotherapy for Prostate Cancer: Detection Rates and Impact on Radiotherapeutic Management. *Int J Radiat Oncol Biol Phys* 2020;108(3):S18.
29. Fendler WP, Calais J, Eiber M, et al. Assessment of ^{68}Ga -PSMA-11 PET Accuracy in Localizing Recurrent Prostate Cancer: A Prospective Single-Arm Clinical Trial. *JAMA Oncol* 2019;5(6):856–863.
30. Meijer D, van Leeuwen PJ, Roberts MJ, et al. External Validation and Addition of Prostate-specific Membrane Antigen Positron Emission Tomography to the Most Frequently Used Nomograms for the Prediction of Pelvic Lymph-node Metastases: an International Multicenter Study. *Eur Urol* 2021;80(2):234–242.
31. Malaspina S, Anttinen M, Taimen P, et al. Response to the Letter to the Editor: Prospective comparison of ^{18}F -PSMA-1007 PET/CT, whole-body MRI and CT in primary nodal staging of unfavourable intermediate- and high-risk prostate cancer. *Eur J Nucl Med Mol Imaging* 2021;48(9):2672–2673.
32. Arslan A, Karaarslan E, Güner AL, Sağlıcan Y, Tuna MB, Kural AR. Comparing the Diagnostic Performance of Multiparametric Prostate MRI Versus ^{68}Ga -PSMA PET-CT in the Evaluation Lymph Node Involvement and Extraprostatic Extension. *Acad Radiol* 2022;29(5):698–704.